Probing the brain with molecular fMRI

HHS Public Access

Author manuscript

Curr Opin Neurobiol. Author manuscript; available in PMC 2019 June 01.

Published in final edited form as:

Curr Opin Neurobiol. 2018 June ; 50: 201–210. doi:10.1016/j.conb.2018.03.009.

Probing the Brain with Molecular fMRI

Souparno Ghosh[1,†], **Peter Harvey**[1,†], **Jacob C. Simon**[1,†], and **Alan Jasanoff**[1,2,3,*]

[1]Department of Biological Engineering, Massachusetts Institute of Technology, 77 Massachusetts Ave., Rm. 16-561, Cambridge, MA 02139

[2]Department of Brain & Cognitive Sciences, Massachusetts Institute of Technology, 77 Massachusetts Ave., Rm. 16-561, Cambridge, MA 02139

[3]Department of Nuclear Science & Engineering, Massachusetts Institute of Technology, 77 Massachusetts Ave., Rm. 16-561, Cambridge, MA 02139

Abstract

One of the greatest challenges of modern neuroscience is to incorporate our growing knowledge of molecular and cellular-scale physiology into integrated, organismic-scale models of brain function in behavior and cognition. Molecular-level functional magnetic resonance imaging (molecular fMRI) is a new technology that can help bridge these scales by mapping defined microscopic phenomena over large, optically-inaccessible regions of the living brain. In this review, we explain how MRI-detectable imaging probes can be used to sensitize noninvasive imaging to mechanistically-significant components of neural processing. We discuss how a combination of innovative probe design, advanced imaging methods, and strategies for brain delivery can make molecular fMRI an increasingly successful approach for spatiotemporally-resolved studies of diverse neural phenomena, perhaps eventually in people.

INTRODUCTION

The landscape of brain research today is divided [1]. On one side is human cognitive neuroscience, which depends on noninvasive whole-brain neuroimaging tools with extraordinary capabilities but limited explanatory power, as exemplified by functional magnetic resonance imaging (fMRI) [2]. On the other side is reductionist neurobiology, which harnesses increasingly powerful but typically invasive techniques that operate on the cellular and molecular levels in animals and model systems [3].

A new technique called “molecular fMRI” has the potential to help bridge this divide. Molecular fMRI is an alternative form of fMRI that monitors brain activity through the use of chemical or genetically-encoded probes designed to sense specific molecular and cellular targets in the brain [4]. Molecular fMRI readouts thus reflect distinct molecular hallmarks of

*Address correspondence to AJ, phone: 617-452-2538, fax: 617-324-1985, jasanoff@mit.edu.

†equal contribution

neural activity, rather than the complex coupling between neural activity and blood flow that underlies conventional hemodynamic fMRI [5]. The imaging probes used in molecular fMRI are analogous to state-of-the-art optical imaging agents like fluorescent dyes and proteins [6], but they influence magnetic signals rather than visible light, and they can be detected in deep brain regions and over wide fields of view that are currently inaccessible to optical methods. For this reason, molecular fMRI may extend the reach of deep tissue activity measurements in animals and eventually allow cellular-level, mechanistically informative neuroimaging in human subjects.

The goals of molecular fMRI technology development are threefold: (1) permit noninvasive analogs of the sorts of optical imaging now possible using tools like GCaMP6 [7]; (2) increase the set of physiological phenomena that can be measured by dynamic imaging in deep tissue and intact brains; and (3) enable molecular-level measurements of brain function at high spatial and temporal resolution in people. Current technology is still far from realizing these goals, but significant progress is being made. Earlier reviews have focused largely on the design principles of molecular fMRI probes, and on technical aspects of probe development and validation [4,8]. Here we adopt a more goal-oriented perspective in discussing recent advances and prospects for molecular fMRI methodologies that could enable neuroscientists of multiple stripes to probe entire brains with molecular precision.

Prospects for emulating optical activity imaging using fMRI

Establishing an MRI-based version of high-resolution optical neuroimaging techniques requires both sensors and imaging methods that are up to the task. A considerable hurdle has been the development of MRI probes for measuring calcium ions, which have long been the favored targets in optical imaging. The first calcium sensor detectable by magnetic resonance techniques was a fluorinated analog of the calcium chelator 1,2-bis-(o-aminophenoxy)ethane-*N,N,N′,N′*-tetraacetic acid) (BAPTA) [9]. Fluorinated BAPTA reports calcium via spectroscopic signals that are too weak to enable imaging of low calcium concentrations under normal circumstances. A clever strategy called chemical exchange saturation transfer (CEST) enabled Bar-Shir *et al.* to partially override this limitation, however [10]. They reported detection of 0.5 μM Ca^{2+} using 500 μM 5,5'-difluoro-BAPTA (Figure 1a), although they required many minutes to acquire images at millimeter-scale resolution *in vitro*.

More easily detectable calcium imaging probes have been synthesized using paramagnetic or superparamagnetic building blocks that incorporate metals like gadolinium, iron, and manganese. The first such probe was a Gd^{3+}-based contrast agent for T_1-weighted MRI, reported by Meade and colleagues in 1999 [11]. It was comparable in size to fluorescent calcium indicators like fura-2 and Oregon Green BAPTA [12,13], and it worked by producing calcium-dependent brightening in T_1-weighted MRI. Many modifications to this original design have since been made, suitable for both addressing intracellular (0–100 μM) and extracellular (0.1–2 mM) calcium concentration ranges in neural tissue [14,15]. In a 2016 paper by Moussaron *et al.* [16], one such agent was injected at a concentration of 10 mM Gd^{3+} into mouse kidney and shown to respond within five minutes to bolus intravenous

injection of 10 μmol $CaCl_2$; this was the first published evidence of functionality for a T_1-based calcium probe *in vivo* (Figure 1b).

Calcium sensors have also been formed by combining calcium-binding actuation domains with magnetic iron oxide nanoparticles [17]; these probes are visualized by T_2-weighted MRI and can function at low levels (~1 μM in calcium binding sites) that are unlikely to perturb endogenous calcium concentrations. Although early nanoparticle probes displayed kinetics on the order of minutes, improved versions achieved responses within a few seconds [18], suitable for functional imaging with temporal resolution comparable to current fMRI techniques (Figure 1c). Very recently, Okada and colleagues introduced a new magnetic calcium-responsive nanoparticle (MaCaReNa) sensor designed to report extracellular Ca^{2+} fluctuations associated with neural activity [19]. Intracranially injected MaCaReNas allowed repeated detection of brain activation in response to chemical and electrophysiological stimuli in rats, constituting the first demonstration of molecular fMRI using an MRI calcium sensor in the living brain. Although response times on the order of seconds were reported in this study, there is still need to improve kinetic properties of the probe, optimize brain delivery, and further characterize the relationships between MaCaReNa-based signals and underlying neural activity patterns. The MaCaReNa probes may already permit meaningful experimental applications of calcium-dependent molecular fMRI in some contexts, however.

In addition to developing suitable imaging agents, emulating optical neuroimaging using MRI requires fast, high-resolution data acquisition methods. The theoretical spatial resolution of MRI is in the 1–10 μm range for biological tissue [20], but approaching this limit with reasonable signal-to-noise ratio (SNR) usually requires scan times longer than an hour [21–23]. A practical standard for fMRI with high spatiotemporal resolution was set by Yu, Koretsky, and colleagues, who demonstrated the possibility of performing hemodynamic functional imaging in rats at the level of single venules and arterioles, resolved with voxel sizes of 100 × 100 × 500 μm and a frame rate of 10 Hz on a 14 T scanner [24] (Figure 2). Strategies for improving SNR per unit time have included reducing the number of data points required per image via a strategy called compressed sensing, which exploits the same principles involved in producing JPEG images [25,26]. A second approach has been to reduce the field of view. In one example, Yu *et al.* achieved fMRI temporal resolution of 50 ms at 11.7 T for voxels of about 50 μm × 1 mm × 1 mm by using line-scanning techniques similar to those sometimes used in ultrafast optical imaging [27]. Finally, it is possible to improve the amount of data acquired per scan by exploiting multicoil detection systems and excitation strategies that allow multiple fields of view to be imaged simultaneously [28,29]. Extrapolating from current benchmarks, a combination of compressed sensing and multicoil imaging should enable video rate fMRI to be performed with isotropic spatial resolutions of about 150 μm at MRI field strengths above 20 T, which are already becoming available for some applications and are expected to be safe for neuroimaging [30].

MRI sensors for additional targets in the brain

Expanding the list of brain processes accessible to imaging is a major goal for the further development of molecular fMRI technology. Neurotransmitters are particularly important targets in this regard. In the most advanced work to date, MRI sensors based on the

paramagnetic metalloprotein P450-BM3h have been employed to map striatal dopamine release patterns elicited by rewarding brain stimulation that simulates drugs of abuse [31] (Figure 3a–c), and to measure changes in serotonin reuptake rates in response to clinically-relevant monoamine transporter blockers such as the antidepressant fluoxetine [32]. Metalloprotein MRI sensors must generally be applied at concentrations above 10 μM in order to affect image contrast substantially, however; they thus exhibit limited analyte sensitivity and can also perturb neurotransmitter dynamics through buffering and slow interaction kinetics (*e.g.* k_{off} = 0.02 s^{-1} for dopamine-sensitive BM3h) [31]. Promising avenues for future work therefore include improvement of these tools, as well as targeting of additional neurotransmitters such as glutamate and γ-aminobutyric acid.

In addition to sensing neurotransmitters, the development of genetic reporters has been a major focus of efforts in the field [33]. Reporters detectable by MRI could permit repeated noninvasive whole-brain imaging of gene expression patterns in single animals, and could therefore prove useful for noninvasive studies of neuroplasticity or activity-dependent processes [34]. The first validated approaches to genetic imaging in MRI used reporter enzyme-activated contrast agents [35], metalloproteins like the iron storage complex ferritin [36,37], or transporters capable of catalyzing intracellular metal accumulation [38–41]. Despite ongoing efforts to improve the functionality of such systems through protein engineering [42–44], none of these methods yet seems to be powerful enough for robust application *in vivo*. Some strategies that rely on intracellular metal accumulation come with the particular pitfall that they can incur oxidative damage or other toxic side effects in cells [45]. An elegant way to sidestep this problem employs the CEST technique for detection of exchangeable protons on diamagnetic species such as labile proton-rich polypeptides or reporter enzyme products [46,47], although detection sensitivity is limited with these approaches as well.

A common theme in the development of neurotransmitter sensors and genetic MRI reporters is the need for improved signal changes. Theoretical studies predict that significant gains in the potency of T_1 and CEST-based contrast agents may be possible [48,49], improving detectability of these species to concentrations below 10 μM. Magnetic nanoparticle probes can already be detected at submicromolar levels, but they exhibit relatively slow response rates. Modeling results suggest routes for improvement of their kinetics however [50,51], and reduction of nanoparticle dimensions will also likely facilitate brain delivery and applications in living tissue. Demonstration of calcium-dependent molecular fMRI using MaCaReNa probes in rat brain [19] further supports the idea that suitably constructed magnetic particle-based sensors could be suitable for functional imaging of neurotransmitters and additional targets *in vivo*.

Several recent studies have explored novel contrast mechanisms that might also provide high sensitivity to molecular targets in the brain [52]. In one approach, water-permeable channels were employed as gene reporters that alter signal in diffusion-weighted MRI scans [53,54]; it might become possible to modulate this signal on a relatively fast timescale by coupling the water permeability of the channels to the presence of analytes of interest. In a second approach, the endogenous phenomenon of neurovascular coupling, which underlies conventional hemodynamic fMRI as well as a host of other functional imaging approaches,

was “hijacked” and employed as a specific readout of enzyme activity and gene expression [55] (Figure 3d–f). The published work employs vasoactive molecules based on calcitonin gene-related peptide (CGRP) as contrast agents that can be detected at nanomolar concentrations when secreted by cells or applied exogenously, but future variants could involve engineering other aspects of vascular biology to report on a wide variety of neural signaling processes.

Given the variety of MRI contrast sources available, an intriguing direction for future technology development might be to combine different sensors for simultaneous measurement of multiple analytes at the same time; this would be analogous to using fluorescent probes with different excitation and emission wavelengths in parallel for optical imaging. CEST contrast is particularly conducive to such multiplexing [56,57], but implementing this for molecular fMRI in practice would increase scan times, reducing the already limited temporal resolution of CEST-based detection methods [50]. Acquisition schemes that simultaneously measure T_1 and T_2 or T_2* relaxation-weighted signals offer the possibility of applying T_1 and T_2 weighting agents in combination [58]. Separating T_1 and T_2 effects from different probes is complicated however by the fact that most relevant contrast agents have some effect on both parameters.

Toward molecular fMRI in humans

Progress with molecular fMRI tools for animal studies is accelerating, but some of the greatest payoffs of this technology may ultimately be achieved in human subjects. It is in only people that molecular fMRI could be applied to examine neural correlates of high level cognitive processes or subjective perceptual experiences in depth; in human patients molecular fMRI could also come to guide diagnosis and treatment of brain diseases by defining new biomarkers or mechanistically significant hallmarks of neural processing. In order to make translation of molecular fMRI methods feasible, two major criteria must be satisfied: (1) completely noninvasive delivery of imaging probes must be possible; and (2) contrast agents must be nontoxic and stable enough for human use.

Noninvasive brain delivery of MRI contrast agents requires a strategy for getting them across the blood-brain barrier (BBB), the system of intercellular connections that keeps most blood-borne substances from penetrating the central nervous system [59]. A leading technique for enabling this uses ultrasound pressure waves, in conjunction with intravenous acoustically-absorbant microbubbles, to transiently disrupt the BBB [60] (Figure 4a–c). Ultrasound-mediated BBB disruption permits analytes of widely varying sizes to enter the brain over a period of roughly one hour following sonication [61]. A recent clinical trial demonstrated successful delivery of chemotherapeutics and MRI contrast agents among a set of fifteen brain tumor patients, proving the potential of ultrasound for delivery of molecular imaging agents in people [62]. Last year, the first clinical trial of ultrasound-mediated BBB opening in Alzheimer’s disease (AD) patients began, with brain delivery of a gadolinium contrast agent again used as the basis for monitoring BBB disruption [63]. If this trial proves successful, then ultrasound-facilitated delivery techniques might prove safe for application in additional neurological patient populations. On the other hand, evidence of inflammation has been reported following transcranial ultrasound in animal models [64], and similar side

effects may also arise in conjunction with older osmotic shock-mediated BBB opening methodology [65]. BBB disruption techniques might therefore prove most suitable for application of molecular fMRI tools in urgent care situations, but could be too risky for application in more healthy subjects.

The safest approaches to brain delivery of molecular fMRI probes would rely on probes that cross the BBB on their own. Spontaneously permeable agents can make use of three pathways for traversing the barrier: passive transport across cell membranes, compatibility with endogenous solute carrier-mediated transport (CMT) systems, or affinity for receptors that mediate trans-BBB transport of macromolecules [66] (Figure 4d). Synthesis of lipophilic MRI contrast agents and sensors is a challenge because most agents incorporate highly polar metal complexes. Some efforts have attempted to circumvent this problem by creating imaging agents based on nonstandard planar aromatic chelators [67]; these were recently demonstrated to penetrate cells and enable detection of intracellular enzymes by MRI [68].

Receptor mediated transport (RMT)-catalyzed brain delivery of imaging agents has been demonstrated by incorporating probes into so-called molecular Trojan horses—molecules that themselves undergo RMT and carry along whatever species are associated with them [69]. The best explored Trojan horse-based approaches involve conjugating agents to proteins that bind to the transferrin and insulin receptors on the BBB (Figure 4e–f). These strategies have been shown to promote safe, high efficiency delivery of antibody derivatives to primate brain [70,71]. Some of the more sensitive MRI agents, such as vasoprobes, might be delivered this way. Higher probe doses might be deliverable by packaging high concentrations into nanoparticles, which could then be conjugated to Trojan horses. In an example of this approach, Koffie *et al.* loaded imaging probes into nanoparticles of polybutyl cyanoacrylate, which are coated *in vivo* by endogenous apolipo-protein E, a substrate for trans-BBB RMT [72]. Following intravenous injection of complexes containing the MRI contrast agent gadobutrol, the authors observed enhancement of T_1-weighted brain image intensity.

If molecular fMRI agents are to be used in people, they must be nontoxic as well as deliverable to the brain. Fortunately, several contrast agent architectures are already approved for human use; these include both iron oxide nanoparticles and small molecule metal chelates, which are used in approximately 30% of all clinical MRI scans [73]. Some gadolinium-based T_1 contrast agents have recently received negative publicity due to the link between Gd^{3+} release and nephrogenic systemic fibrosis, a rare but devastating disorder [74]; additional reports have documented metal accumulation in the brains of some MRI subjects [75]. The more stable macrocyclic gadolinium agents are unlikely to display this problem however [76], and there are also now substantial efforts to develop gadolinium-free T_1 agents that achieve their effects using paramagnetic manganese, iron, or organic radicals [77–79].

Incorporation of clinically acceptable building blocks into responsive agents for neuroimaging could create new risks, so further clinical testing will be required before human use of such agents. It seems unlikely that this process will be motivated primarily by

the potential benefits of molecular fMRI agents for basic research. Instead, clinical testing and approval of molecular fMRI tools will be driven by medical needs. Diagnostic applications of molecular neuroimaging agents can easily be imagined. For example, calcium sensors could be powerful tools for measuring signaling abnormalities implicated in brain diseases such as autism and Alzheimer's disease [80,81]. Neurotransmitter sensors could be useful for monitoring therapy in disorders that affect particular neurochemical systems, like Parkinson's disease or major depression. This kind of context—where molecular fMRI agents are used as "companion diagnostics" to assess efficacy of drugs or other biological treatments—could in fact provide a general route for clinical adoption of novel neuroimaging probes [82].

Conclusions

Molecular fMRI methodology is already being applied for unprecedented mesoscale mapping of neurophysiological processes in animals, and could eventually be deployed in people. Although applications to date are restricted by the relative insensitivity of most existing responsive imaging probes, substantial efforts are now underway to improve probe characteristics, facilitate brain delivery, explore novel MRI contrast mechanisms, and expand the repertoire of molecular targets that can be sensed in the nervous system. There is much work to be done, but the need for this research is outstanding. Molecular fMRI and related neuroimaging techniques offer special promise for improving our ability to relate large-scale integrative functions of the brain to mechanistically informative molecular and cellular variables. Establishing these relationships is essential for explaining how low-level neurophysiology guides high-level behavior and cognition, a problem around which both sides of our divided field can come together.

Acknowledgments

This work was supported by grants from the National Institutes of Health (R01 DA038642, R24 MH109081, U01 NS103470, and R21 DA044748), the MGH-MIT Grant Challenge program, and the Simons Center for the Social Brain to APJ. SG was funded by an HHMI International Student Research Fellowship and Sheldon Razin Fellowship from the McGovern Institute for Brain Research. JCS was supported by NIH training grant T32 EB019940, and PH was supported by a Wellcome Trust-MIT Postdoctoral Fellowship. The authors thank Xin Yu and Goran Angelovski for sharing high resolution figure panels.

Abbreviations

BAPTA	1,2-Bis-(o-Aminophenoxy)ethane-*N,N,N′,N′*-Tetraacetic Acid)
BBB	Blood-Brain Barrier
CGRP	Calcitonin Gene-Related Peptide
CMT	Carrier-Mediated Transport
CEST	Chemical Exchange Saturation Transfer
fMRI	Functional Magnetic Resonance Imaging
MRI	Magnetic Resonance Imaging

RMT	Receptor-Mediated Transport
SNR	Signal-to-Noise Ratio

References

1. Badre D, Frank MJ, Moore CI. Interactionist Neuroscience. Neuron. 2015; 88:855–860. [PubMed: 26637794]
2. Ugurbil K. What is feasible with imaging human brain function and connectivity using functional magnetic resonance imaging. Philos Trans R Soc Lond B Biol Sci. 2016; 371
3. Jorgenson LA, Newsome WT, Anderson DJ, Bargmann CI, Brown EN, Deisseroth K, Donoghue JP, Hudson KL, Ling GS, MacLeish PR, et al. The BRAIN Initiative: developing technology to catalyse neuroscience discovery. Philos Trans R Soc Lond B Biol Sci. 2015; 370
4. Bartelle BB, Barandov A, Jasanoff A. Molecular fMRI. J Neurosci. 2016; 36:4139–4148. [PubMed: 27076413]
5. Hillman EM. Coupling mechanism and significance of the BOLD signal: a status report. Annu Rev Neurosci. 2014; 37:161–181. [PubMed: 25032494]
6. Lin MZ, Schnitzer MJ. Genetically encoded indicators of neuronal activity. Nat Neurosci. 2016; 19:1142–1153. [PubMed: 27571193]
7. Chen TW, Wardill TJ, Sun Y, Pulver SR, Renninger SL, Baohan A, Schreiter ER, Kerr RA, Orger MB, Jayaraman V, et al. Ultrasensitive fluorescent proteins for imaging neuronal activity. Nature. 2013; 499:295–300. [PubMed: 23868258]
8. Hsieh V, Jasanoff A. Bioengineered probes for molecular magnetic resonance imaging in the nervous system. ACS Chem Neurosci. 2012; 3:593–602. [PubMed: 22896803]
9. Smith GA, Hesketh RT, Metcalfe JC, Feeney J, Morris PG. Intracellular calcium measurements by ^{19}F NMR of fluorine-labeled chelators. Proc Natl Acad Sci U S A. 1983; 80:7178–7182. [PubMed: 6417665]
10. Bar-Shir A, Gilad AA, Chan KW, Liu G, van Zijl PC, Bulte JW, McMahon MT. Metal ion sensing using ion chemical exchange saturation transfer ^{19}F magnetic resonance imaging. J Am Chem Soc. 2013; 135:12164–12167. [PubMed: 23905693]
11. Li W, Fraser SE, Meade TJ. A calcium-sensitive magnetic resonance imaging contrast agent. J. Am. Chem. Soc. 1999; 121:1413–1414.
12. Grynkiewicz G, Poenie M, Tsien RY. A new generation of Ca^{2+} indicators with greatly improved fluorescence properties. J Biol Chem. 1985; 260:3440–3450. [PubMed: 3838314]
13. Johnson ID, Spence M, editorsThe Molecular Probes Handbook: A Guide to Fluorescent Probes and Labeling Technologies. 11. Carlsbad, CA: Life Technologies Corp.; 2010.
14. Que EL, Chang CJ. Responsive magnetic resonance imaging contrast agents as chemical sensors for metals in biology and medicine. Chem Soc Rev. 2010; 39:51–60. [PubMed: 20023836]
15. Angelovski G. Heading toward Macromolecular and Nanosized Bioresponsive MRI Probes for Successful Functional Imaging. Acc Chem Res. 2017; 50:2215–2224. [PubMed: 28841293]

*16. Moussaron A, Vibhute S, Bianchi A, Gunduz S, Kotb S, Sancey L, Motto-Ros V, Rizzitelli S, Cremillieux Y, Lux F, et al. Ultrasmall Nanoplatforms as Calcium-Responsive Contrast Agents for Magnetic Resonance Imaging. Small. 2015; 11:4900–4909. The authors presented the first evidence of MRI-based calcium sensing *in vivo* using a calcium-sensitive T_1 contrast agent. The agent was injected into kidney and responses were triggered by a bolus dose of intravascular $CaCl_2$. [PubMed: 26179212]

17. Atanasijevic T, Shusteff M, Fam P, Jasanoff A. Calcium-sensitive MRI contrast agents based on superparamagnetic iron oxide nanoparticles and calmodulin. Proc Natl Acad Sci U S A. 2006; 103:14707–14712. [PubMed: 17003117]
18. Rodriguez E, Lelyveld VS, Atanasijevic T, Okada S, Jasanoff A. Magnetic nanosensors optimized for rapid and reversible self-assembly. Chem Commun (Camb). 2014; 50:3595–3598. [PubMed: 24566735]

**19. Okada S, Bartelle BB, Li N, Lee J, Rodriguez E, Melican J, Jasanoff A. Calcium-dependent molecular fMRI using a magnetic nanosensor. Nat Nanotechnol. 2018 accepted. This paper presents the first evidence of calcium-dependent molecular fMRI in the living brain, using a magnetic particle-based sensor for extracellular Ca^{2+} called MaCaReNa. The probe enables detection of responses to chemical and electrical brain stimulation, with response times on the order of seconds in intracranially injected rats.

20. Callaghan PT. Principles of Nuclear Magnetic Resonance Microscopy. Oxford, UK: Oxford University Press; 1993.

21. Lee SC, Kim K, Kim J, Yi JH, Lee S, Cheong C. MR microscopy of micron scale structures. Magn Reson Imaging. 2009; 27:828–833. [PubMed: 19282120]

22. Flint JJ, Lee CH, Hansen B, Fey M, Schmidig D, Bui JD, King MA, Vestergaard-Poulsen P, Blackband SJ. Magnetic resonance microscopy of mammalian neurons. Neuroimage. 2009; 46:1037–1040. [PubMed: 19286461]

23. Lee CH, Blackband SJ, Fernandez-Funez P. Visualization of synaptic domains in the Drosophila brain by magnetic resonance microscopy at 10 micron isotropic resolution. Sci Rep. 2015; 5:8920. [PubMed: 25753480]

**24. Yu X, He Y, Wang M, Merkle H, Dodd SJ, Silva AC, Koretsky AP. Sensory and optogenetically driven single-vessel fMRI. Nat Methods. 2016; 13:337–340. This paper demonstrates the high spatiotemporal resolution accessible using current high field fMRI techniques in animals. The authors were able to resolve hemodynamic responses in individual blood vessels in rat somatosensory cortex. [PubMed: 26855362]

25. Lustig M, Donoho D, Pauly JM. Sparse MRI: The application of compressed sensing for rapid MR imaging. Magn Reson Med. 2007; 58:1182–1195. [PubMed: 17969013]

26. Fang Z, Van Le N, Choy M, Lee JH. High spatial resolution compressed sensing (HSPARSE) functional MRI. Magn Reson Med. 2016; 76:440–455. [PubMed: 26511101]

27. Yu X, Qian C, Chen DY, Dodd SJ, Koretsky AP. Deciphering laminar-specific neural inputs with line-scanning fMRI. Nat Methods. 2014; 11:55–58. [PubMed: 24240320]

28. Larkman DJ, Hajnal JV, Herlihy AH, Coutts GA, Young IR, Ehnholm G. Use of multicoil arrays for separation of signal from multiple slices simultaneously excited. J Magn Reson Imaging. 2001; 13:313–317. [PubMed: 11169840]

29. Barth M, Breuer F, Koopmans PJ, Norris DG, Poser BA. Simultaneous multislice (SMS) imaging techniques. Magn Reson Med. 2016; 75:63–81. [PubMed: 26308571]

30. Budinger TF, Bird MD. MRI and MRS of the human brain at magnetic fields of 14T to 20T: Technical feasibility, safety, and neuroscience horizons. Neuroimage. 2017

**31. Lee T, Cai LX, Lelyveld VS, Hai A, Jasanoff A. Molecular-level functional magnetic resonance imaging of dopaminergic signaling. Science. 2014; 344:533–535. This paper presents the first demonstration of molecular fMRI, using a neurotransmitter-sensitive contrast agent to map dopamine release over the striatum in rats, in response to reward-related brain stimulation. [PubMed: 24786083]

*32. Hai A, Cai LX, Lee T, Lelyveld VS, Jasanoff A. Molecular fMRI of Serotonin Transport. Neuron. 2016; 92:754–765. This study demonstrates molecular fMRI-based mapping of neurotransmitter removal from the brain. A serotonin-bound metalloprotein probe was injected used to measure localized changes in serotonin reuptake in striatum, as well as changes induced by serotonin and dopamine transporter inhibitors such as Prozac. [PubMed: 27773583]

33. Srivastava AK, Kadayakkara DK, Bar-Shir A, Gilad AA, McMahon MT, Bulte JW. Advances in using MRI probes and sensors for in vivo cell tracking as applied to regenerative medicine. Dis Model Mech. 2015; 8:323–336. [PubMed: 26035841]

34. Kovacs KJ. Measurement of immediate-early gene activation—c-fos and beyond. J Neuroendocrinol. 2008; 20:665–672. [PubMed: 18601687]

35. Louie AY, Huber MM, Ahrens ET, Rothbacher U, Moats R, Jacobs RE, Fraser SE, Meade TJ. In vivo visualization of gene expression using magnetic resonance imaging. Nat Biotechnol. 2000; 18:321–325. [PubMed: 10700150]

36. Cohen B, Dafni H, Meir G, Harmelin A, Neeman M. Ferritin as an endogenous MRI reporter for noninvasive imaging of gene expression in C6 glioma tumors. Neoplasia. 2005; 7:109–117. [PubMed: 15802016]

37. Genove G, DeMarco U, Xu H, Goins WF, Ahrens ET. A new transgene reporter for in vivo magnetic resonance imaging. Nat Med. 2005; 11:450–454. [PubMed: 15778721]

38. Weissleder R, Moore A, Mahmood U, Bhorade R, Benveniste H, Chiocca EA, Basilion JP. In vivo magnetic resonance imaging of transgene expression. Nat Med. 2000; 6:351–355. [PubMed: 10700241]

39. Zurkiya O, Chan AW, Hu X. MagA is sufficient for producing magnetic nanoparticles in mammalian cells, making it an MRI reporter. Magn Reson Med. 2008; 59:1225–1231. [PubMed: 18506784]

40. Goldhawk DE, Lemaire C, McCreary CR, McGirr R, Dhanvantari S, Thompson RT, Figueredo R, Koropatnick J, Foster P, Prato FS. Magnetic resonance imaging of cells overexpressing MagA, an endogenous contrast agent for live cell imaging. Mol Imaging. 2009; 8:129–139. [PubMed: 19723470]

41. Bartelle BB, Szulc KU, Suero-Abreu GA, Rodriguez JJ, Turnbull DH. Divalent metal transporter, DMT1: a novel MRI reporter protein. Magn Reson Med. 2013; 70:842–850. [PubMed: 23065715]

42. Iordanova B, Robison CS, Ahrens ET. Design and characterization of a chimeric ferritin with enhanced iron loading and transverse NMR relaxation rate. J Biol Inorg Chem. 2010; 15:957–965. [PubMed: 20401622]

43. Matsumoto Y, Chen R, Anikeeva P, Jasanoff A. Engineering intracellular biomineralization and biosensing by a magnetic protein. Nat Commun. 2015; 6:8721. [PubMed: 26522873]

44. Radoul M, Lewin L, Cohen B, Oren R, Popov S, Davidov G, Vandsburger MH, Harmelin A, Bitton R, Greneche JM, et al. Genetic manipulation of iron biomineralization enhances MR relaxivity in a ferritin-M6A chimeric complex. Sci Rep. 2016; 6:26550. [PubMed: 27211820]

45. Pereira SM, Williams SR, Murray P, Taylor A. MS-1 magA: Revisiting Its Efficacy as a Reporter Gene for MRI. Mol Imaging. 2016; 15

46. Gilad AA, McMahon MT, Walczak P, Winnard PT Jr, Raman V, van Laarhoven HW, Skoglund CM, Bulte JW, van Zijl PC. Artificial reporter gene providing MRI contrast based on proton exchange. Nat Biotechnol. 2007; 25:217–219. [PubMed: 17259977]

47. Bar-Shir A, Liang Y, Chan KW, Gilad AA, Bulte JW. Supercharged green fluorescent proteins as bimodal reporter genes for CEST MRI and optical imaging. Chem Commun (Camb). 2015; 51:4869–4871. [PubMed: 25697683]

48. Woods M, Woessner DE, Sherry AD. Paramagnetic lanthanide complexes as PARACEST agents for medical imaging. Chem Soc Rev. 2006; 35:500–511. [PubMed: 16729144]

49. Caravan P, Farrar CT, Frullano L, Uppal R. Influence of molecular parameters and increasing magnetic field strength on relaxivity of gadolinium- and manganese-based T_1 contrast agents. Contrast Media Mol Imaging. 2009; 4:89–100. [PubMed: 19177472]

50. Shapiro MG, Atanasijevic T, Faas H, Westmeyer GG, Jasanoff A. Dynamic imaging with MRI contrast agents: quantitative considerations. Magn Reson Imaging. 2006; 24:449–462. [PubMed: 16677952]

51. Matsumoto Y, Jasanoff A. T_2 relaxation induced by clusters of superparamagnetic nanoparticles: Monte Carlo simulations. Magn Reson Imaging. 2008; 26:994–998. [PubMed: 18479873]

52. Mukherjee A, Davis HC, Ramesh P, Lu GJ, Shapiro MG. Biomolecular MRI reporters: Evolution of new mechanisms. Prog Nucl Magn Reson Spectrosc. 2017; 102–103:32–42.

*53. Mukherjee A, Wu D, Davis HC, Shapiro MG. Non-invasive imaging using reporter genes altering cellular water permeability. Nat Commun. 2016; 7:13891. The authors introduce the use of the water channel aquaporin as a gene reporter in diffusion-weighted MRI. Results show that expression of aquaporin in as few as 10% of cells in a population can be detected. [PubMed: 28008959]

*54. Schilling F, Ros S, Hu DE, D'Santos P, McGuire S, Mair R, Wright AJ, Mannion E, Franklin RJ, Neves AA, et al. MRI measurements of reporter-mediated increases in transmembrane water exchange enable detection of a gene reporter. Nat Biotechnol. 2017; 35:75–80. The authors use the urea transporter UT-B as a water-permeable gene reporter for diffusion-weighted MRI. They

show that lentiviral-mediated UT-B expression in brain tissue induces discernable contrast effects. [PubMed: 27918546]

*55. Desai M, Slusarczyk AL, Chapin A, Barch M, Jasanoff A. Molecular imaging with engineered physiology. Nat Commun. 2016; 7:13607. Probes based on the vasoactive peptide CGRP were designed and employed to couple specific molecular events, like enzyme activity and gene expression, to changes in blood flow. Vasoactive probes can be detected at concentrations 1,000-fold lower than conventional gadolinium-based MRI agents. [PubMed: 27910951]

56. Bar-Shir A, Yadav NN, Gilad AA, van Zijl PC, McMahon MT, Bulte JW. Single ^{19}F probe for simultaneous detection of multiple metal ions using miCEST MRI. J Am Chem Soc. 2015; 137:78–81. [PubMed: 25523816]

57. Finney KNA, Harnden AC, Rogers NJ, Senanayake PK, Blamire AM, O'Hogain D, Parker D. Simultaneous Triple Imaging with Two PARASHIFT Probes: Encoding Anatomical, pH and Temperature Information using Magnetic Resonance Shift Imaging. Chemistry. 2017; 23:7976–7989. [PubMed: 28378890]

58. Metere R, Kober T, Moller HE, Schafer A. Simultaneous Quantitative MRI Mapping of T_1, T_2* and Magnetic Susceptibility with Multi-Echo MP2RAGE. PLoS One. 2017; 12:e0169265. [PubMed: 28081157]

59. Pardridge WM. CSF, blood-brain barrier, and brain drug delivery. Expert Opinion on Drug Delivery. 2016; 13:963–975. [PubMed: 27020469]

60. Aryal M, Arvanitis CD, Alexander PM, McDannold N. Ultrasound-mediated blood–brain barrier disruption for targeted drug delivery in the central nervous system. Advanced Drug Delivery Reviews. 2014; 72:94–109. [PubMed: 24462453]

61. Poon C, McMahon D, Hynynen K. Noninvasive and targeted delivery of therapeutics to the brain using focused ultrasound. Neuropharmacology. 2017; 120:20–37. [PubMed: 26907805]

**62. Carpentier A, Canney M, Vignot A, Reina V, Beccaria K, Horodyckid C, Karachi C, Leclercq D, Lafon C, Chapelon JY, et al. Clinical trial of blood-brain barrier disruption by pulsed ultrasound. Sci Transl Med. 2016; 8 The authors report results from a clinical trial of repeated ultrasound-based BBB-disruption using implanted transducers in cancer patients. Gadolinium-based MRI contrast agents were used to visualize BBB disruption, demonstrating feasibility of this technique for delivering imaging agents to the human brain.

63. InSightec. Blood-Brain-Barrier Opening Using Focused Ultrasound With IV Contrast Agents in Patients With Early Alzheimer's Disease. ClinicalTrials.gov. 2017 NCT02986932.

64. Kovacs ZI, Kim S, Jikaria N, Qureshi F, Milo B, Lewis BK, Bresler M, Burks SR, Frank JA. Disrupting the blood-brain barrier by focused ultrasound induces sterile inflammation. Proc Natl Acad Sci U S A. 2017; 114:E75–E84. [PubMed: 27994152]

65. Rapoport SI. Osmotic opening of the blood-brain barrier: Principles, mechanism, and therapeutic applications. Cell Mol Neurobiol. 2000; 20:217–230. [PubMed: 10696511]

66. Lajoie JM, Shusta EV. Targeting receptor-mediated transport for delivery of biologics across the blood-brain barrier. Annu Rev Pharmacol Toxicol. 2015; 55:613–631. [PubMed: 25340933]

67. Zhang XA, Lovejoy KS, Jasanoff A, Lippard SJ. Water-soluble porphyrins as a dual-function molecular imaging platform for MRI and fluorescence zinc sensing. Proc Natl Acad Sci U S A. 2007; 104:10780–10785. [PubMed: 17578918]

68. Barandov A, Bartelle BB, Gonzalez BA, White WL, Lippard SJ, Jasanoff A. Membrane-Permeable Mn(III) Complexes for Molecular Magnetic Resonance Imaging of Intracellular Targets. J Am Chem Soc. 2016; 138:5483–5486. [PubMed: 27088782]

69. Pardridge WM. Re-engineering biopharmaceuticals for delivery to brain with molecular Trojan horses. Bioconjug Chem. 2008; 19:1327–1338. [PubMed: 18547095]

**70. Yu YJ, Atwal JK, Zhang Y, Tong RK, Wildsmith KR, Tan C, Bien-Ly N, Hersom M, Maloney JA, Meilandt WJ, et al. Therapeutic bispecific antibodies cross the blood-brain barrier in nonhuman primates. Sci Transl Med. 2014; 6:261ra154. This paper demonstrates the successful use of bispecific antibodies optimized for transferrin receptor binding as BBB-permeable therapeutics to reduce a marker of Alzheimer's disease in monkeys. Similar strategies could be powerful tools for delivering molecular fMRI probes.

71. Boado RJ, Hui EKW, Lu JZ, Pardridge WM. Insulin Receptor Antibody-Iduronate 2-Sulfatase Fusion Protein: Pharmacokinetics, Anti-Drug Antibody, and Safety Pharmacology in Rhesus Monkeys. Biotechnol Bioeng. 2014; 111:2317–2325. [PubMed: 24889100]
72. Koffie RM, Farrar CT, Saidi LJ, William CM, Hyman BT, Spires-Jones TL. Nanoparticles enhance brain delivery of blood-brain barrier-impermeable probes for in vivo optical and magnetic resonance imaging. Proc Natl Acad Sci U S A. 2011; 108:18837–18842. [PubMed: 22065785]
73. Botta M. Metal-based MRI probes. Eur J Inorg Chem. 2012; 2012:1873–1874.
74. Bennett CL, Qureshi ZP, Sartor AO, Norris LB, Murday A, Xirasagar S, Thomsen HS. Gadolinium-induced nephrogenic systemic fibrosis: the rise and fall of an iatrogenic disease. Clin Kidney J. 2012; 5:82–88. [PubMed: 22833806]
75. Kanda T, Fukusato T, Matsuda M, Toyoda K, Oba H, Kotoku J, Haruyama T, Kitajima K, Furui S. Gadolinium-based Contrast Agent Accumulates in the Brain Even in Subjects without Severe Renal Dysfunction: Evaluation of Autopsy Brain Specimens with Inductively Coupled Plasma Mass Spectroscopy. Radiology. 2015; 276:228–232. [PubMed: 25942417]
76. Kanal E. Gadolinium based contrast agents (GBCA): Safety overview after 3 decades of clinical experience. Magn Reson Imaging. 2016; 34:1341–1345. [PubMed: 27608608]
77. Gale EM, Atanasova IP, Blasi F, Ay I, Caravan P. A Manganese Alternative to Gadolinium for MRI Contrast. J Am Chem Soc. 2015; 137:15548–15557. [PubMed: 26588204]
78. Wei H, Bruns OT, Kaul MG, Hansen EC, Barch M, Wisniowska A, Chen O, Chen Y, Li N, Okada S, et al. Exceedingly small iron oxide nanoparticles as positive MRI contrast agents. Proc Natl Acad Sci U S A. 2017; 114:2325–2330. [PubMed: 28193901]
79. Nguyen HVT, Chen QX, Paletta JT, Harvey P, Jiang Y, Zhang H, Boska MD, Ottaviani MF, Jasanoff A, Rajca A, et al. Nitroxide-Based Macromolecular Contrast Agents with Unprecedented Transverse Relaxivity and Stability for Magnetic Resonance Imaging of Tumors. ACS Cent Sci. 2017; 3:800–811. [PubMed: 28776023]
80. Krey JF, Dolmetsch RE. Molecular mechanisms of autism: a possible role for Ca2+ signaling. Curr Opin Neurobiol. 2007; 17:112–119. [PubMed: 17275285]
81. Berridge MJ. Calcium regulation of neural rhythms, memory and Alzheimer's disease. J Physiol. 2014; 592:281–293. [PubMed: 23753528]
82. Van Heertum RL, Scarimbolo R, Ford R, Berdougo E, O'Neal M. Companion diagnostics and molecular imaging-enhanced approaches for oncology clinical trials. Drug Des Devel Ther. 2015; 9:5215–5223.
83. Brustad EM, Lelyveld VS, Snow CD, Crook N, Jung ST, Martinez FM, Scholl TJ, Jasanoff A, Arnold FH. Structure-guided directed evolution of highly selective P450-based magnetic resonance imaging sensors for dopamine and serotonin. J Mol Biol. 2012; 422:245–262. [PubMed: 22659321]

HIGHLIGHTS

- Molecular fMRI combines noninvasive imaging with target-sensitive molecular probes.
- Ca^{2+}-sensitive probes and fast fMRI methods could emulate optical calcium imaging.
- Additional probes target neurochemicals and proteins via multiple contrast mechanisms.
- Brain delivery techniques and clinical compatibility raise prospects for human use.

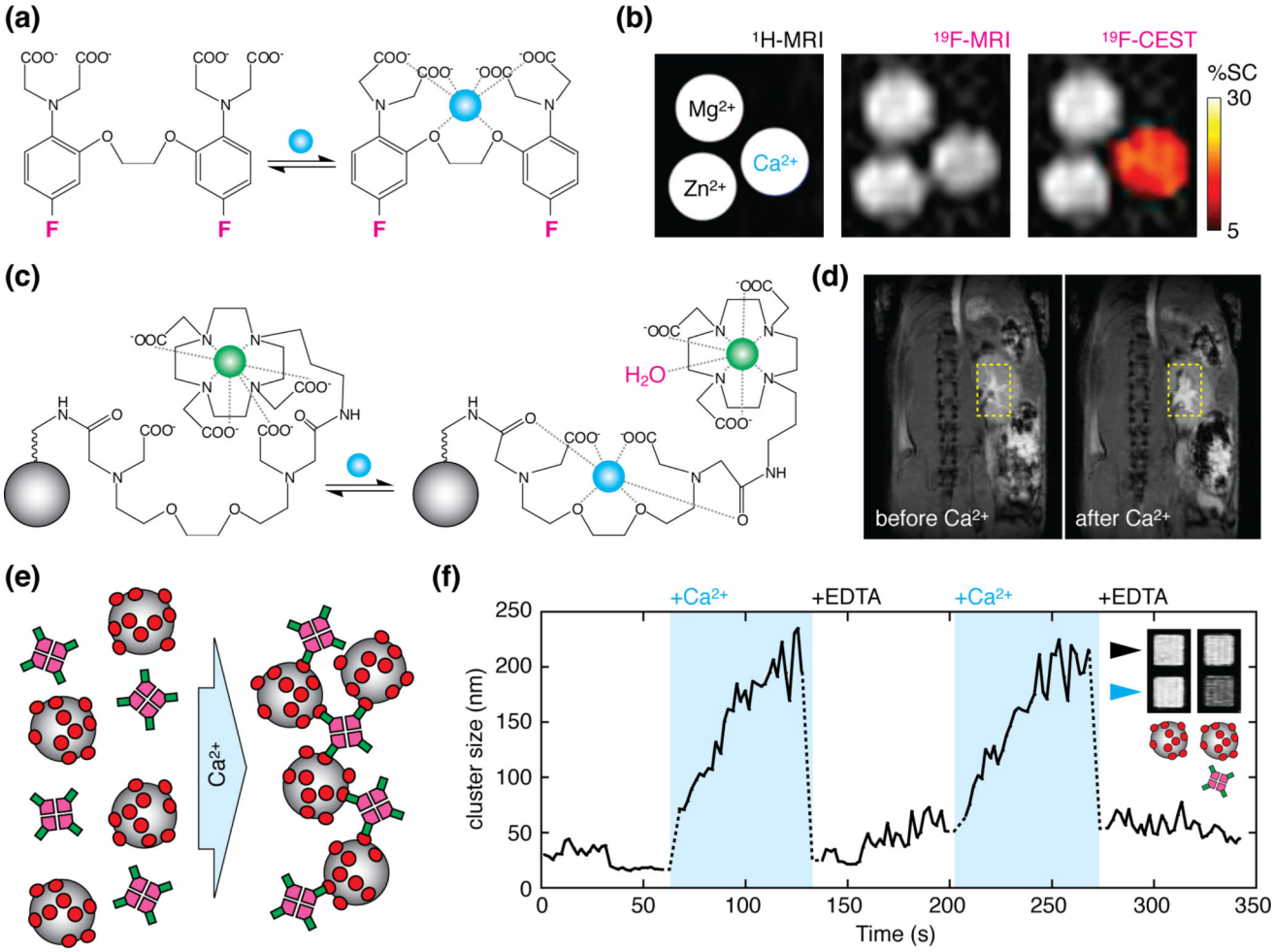

Figure 1.

Calcium sensors potentially suitable for molecular fMRI. **(a)** The 5,5'-difluoro-BAPTA imaging agent used in the approach of ref. [10]. Calcium binding (blue) causes reversible changes in the electronic structure of the agent, and shift the spectroscopic signals associated with the fluorine atoms (magenta). **(b)** Standard proton MRI scan (left), fluorine MRI scan (middle), and fluorine MRI with CEST contrast (right) showing fluorinated BAPTA in the presence of calcium, magnesium, or zinc ions, as indicated in the left panel. Only calcium induces substantial signal change in the CEST image, allowing specific detection of calcium using the agent. **(c)** A gadolinium-based calcium sensor described in ref. [16]. In the presumed mechanism of this probe, one or more of the ligands that coordinate Gd^{3+} (green) in the calcium-free form (left) is sequestered upon calcium binding (right), freeing up additional sites for water molecules (magenta) to interact with Gd^{3+} and induce T_1 MRI contrast enhancement. Conjugation of the agent to a nanoparticle scaffold (gray, not to scale) increases retention time of the agent in tissue. **(d)** MRI contrast change following injection of the probe into mouse kidney, before (left) *vs.* after (right) stimulation with intravenous $CaCl_2$. **(e)** Mechanism of calcium-responsive magnetic nanoparticle sensors in ref. [18]. Clustering of the nanoparticles (gray) is driven by polydendate interactions between calmodulin (red) and a calmodulin-binding peptide (green) attached to a tetrameric

molecular scaffold (magenta). **(f)** Reversible clustering and declustering is measured within seconds of exposure of the sensors to excess Ca^{2+} or EDTA. Inset shows substantial T_2-weighted MRI signal differences measured between EDTA (black arrowhead) and calcium-enriched (blue arrowhead) conditions for nonfunctional control nanoparticles (left) or functional bicomponent sensors (right).

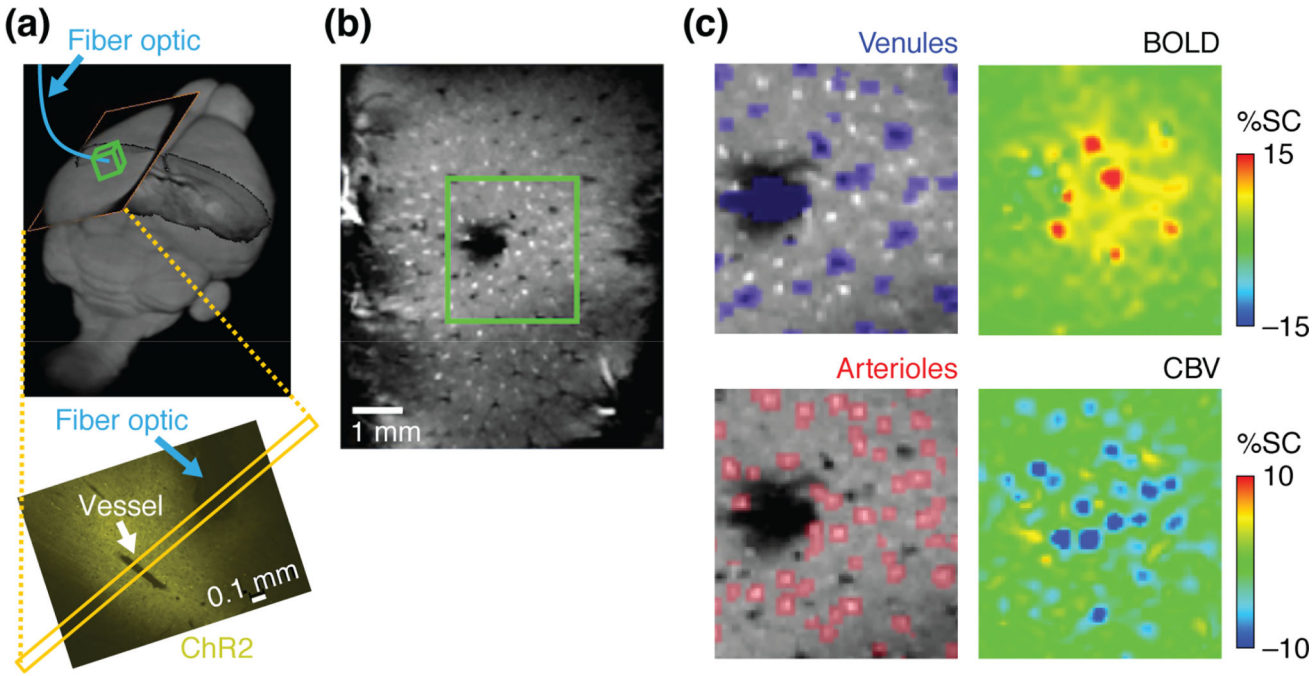

Figure 2.

Hemodynamic fMRI of neural activity signatures resolved at high spatiotemporal resolution. **(a)** Yu *et al.* [24] expressed channelrhodopsin-2 (ChR2) in rat somatosensory cortex and evoked neural responses using optogenetic stimulation via an implanted fiber (blue). Top panel shows orientation of MRI scans in (b–d) and bottom panel shows ChR2 expression pattern in a perpendicular slice. **(b)** A technique called multi-gradient imaging was used to identify single vessels based on contrast signatures in high resolution MRI scans (field of view corresponds to yellow slices in (a)). **(c)** Features in two forms of hemodynamic fMRI —blood oxygen level-dependent contrast (BOLD, top right) and cerebral blood volume-dependent contrast (CBV, bottom right)—could be correlated with regions identified as venules (top left) or arterioles (bottom left) based on data as in (b) (green boxed region). Figure adapted from ref. [24].

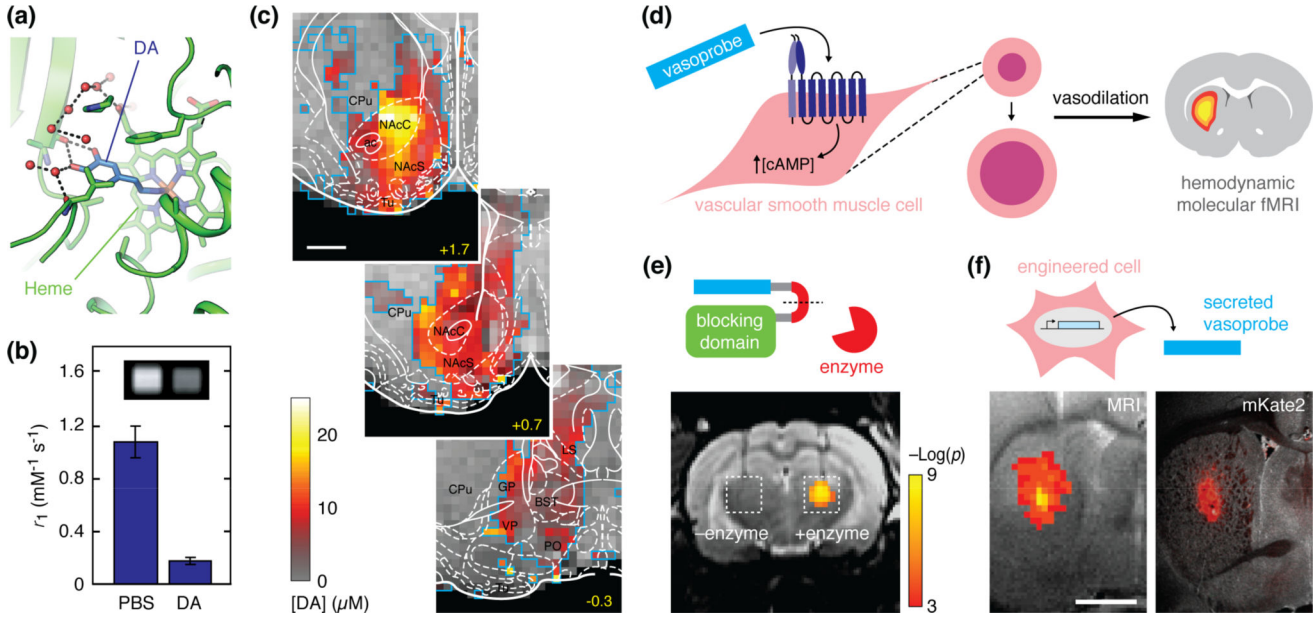

Figure 3.

Molecular fMRI using polypeptide-based imaging agents. **(a)** Structure of a P450-BM3h variant engineered by Brustad *et al.* [83] for selective sensing of the neurotransmitter dopamine in T_1-weighted MRI. The sensing mechanism arises from the ability of dopamine (DA, blue) binding to regulate water access to the paramagnetic heme group (green label) in the core of the protein. **(b)** Dopamine binding to the P450 derivative alters the strength (relaxivity) of the contrast agent, as shown by *in vitro* measurements in PBS and dopamine-containing buffers; inset shows corresponding MRI images. **(c)** Quantitative mapping of dopamine release in rat ventral striatum, elicited by MFB stimulation in the experiments of Lee *et al.* [31]. Panels depict anatomical MRI (grayscale) and atlas divisions (white) in three striatal slices of 1 mm thickness, with color overlay indicating peak dopamine release concentrations determined from raw MRI signal time courses. Scale bar = 2 mm; adapted from ref. [31]. **(d)** Strategy of hijacking hemodynamic responses using molecular agents. Vasoprobes such as the potent vasodilator CGRP agonize receptors on vascular smooth muscle cells (left), promoting relaxation and vasodilation (middle), and leading to changes in blood flow that give rise to MRI signals detectable by hemodynamic molecular fMRI, as well as other imaging techniques. **(e)** Application of vasoprobe-based molecular imaging for detecting enzyme activity. The schematic (top) shows that a caged vasoprobe is inhibited by a blocking domain; in the presence of an enzyme (red), the blocking domain is removed by cleavage of recognition sequence connecting the two (red line segment). The example at bottom demonstrates this principle applied to detection of the protease caspase-3. Enzyme cleaved (right) but not uncleaved (left) probe produces engineered hemodynamic responses upon injection into rat brain, permitting visualization by hemodynamic MRI. Scale indicates statistical significance of the detection. **(f)** Vasoprobes can function as gene reporters by being expressed and secreted from genetically engineered cells (top). Engineered CGRP-expressing human embryonic kidney cells were implanted into rat brain and could be detected by T_2-weighted MRI after 24 hours (bottom left). MRI signal changes coincided with co-expression of a fluorescent protein (mKate), visualized by postmortem histology

(bottom right). Control cells not expressing the vasoprobe did not produce substantial MRI signatures. Scale bar = 2 mm; (d–f) adapted from ref. [55].

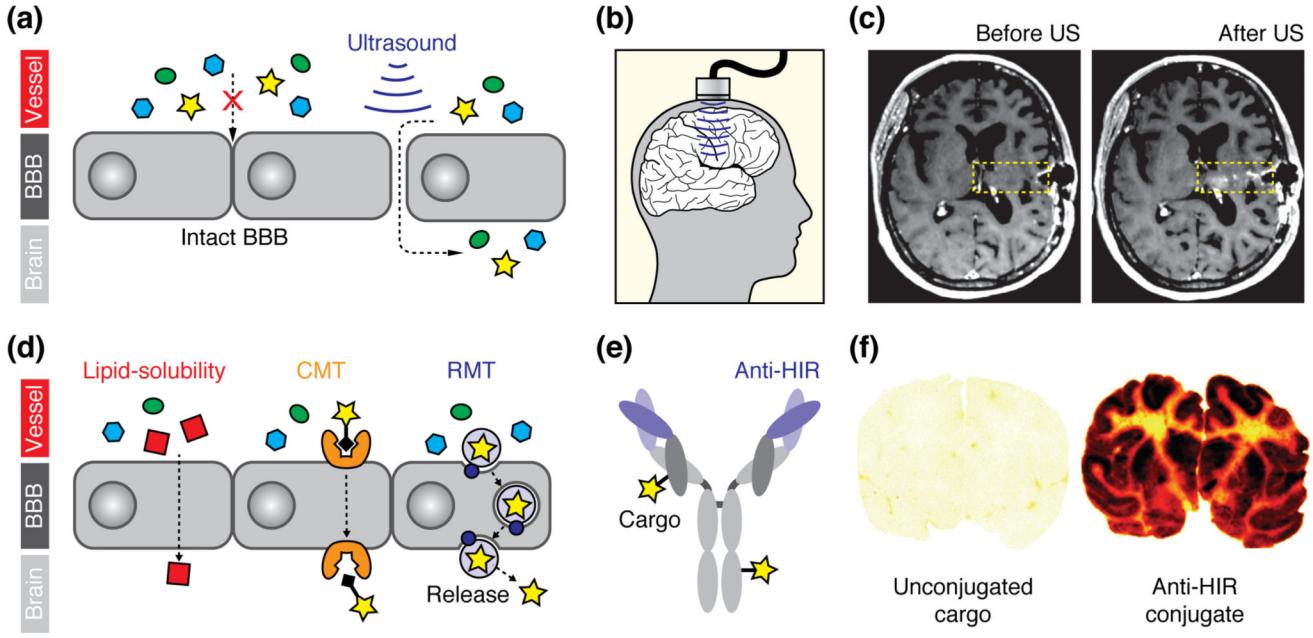

Figure 4.

Delivery of imaging probes across the blood-brain barrier (BBB). (**a**) Simplified schematic demonstrating the opening of the tight junctions between the endothelial cells of the BBB upon application of ultrasound waves in conjunction with intravascular microbubbles (bubbles not shown). Penetration of multiple blood-born species (colored shapes) following BBB disruption takes place, without specificity for imaging reporters *per se*. (**b**) Kovacs *et al*. [64] demonstrated the use of an implantable ultrasound transducer to transiently open the BBB of cancer patients in a clinical trial. (**c**) A gadolinium-based MRI contrast agent was intravenously administered to monitor BBB opening; leakage of the contrast agent into the brain into the sonicated region (yellow box) can be discerned by comparing images acquired before (left) *vs*. after (right) sonication. Figure adapted from ref. 64. (**d**) Mechanisms of spontaneous BBB penetration by imaging agents: (left) transcellular diffusion by lipophilic molecules (red); (middle) carrier-mediated transport (CMT) of imaging agents (star) attached to CMT substrates (black diamond); and (right) and receptor-mediated transport (RMT) of receptor-targeted complexes (light purple circle) incorporating an imaging agent (star), which in some cases may be released once the complex enters the brain. (**e**) Diagram of a typical Trojan horse construct based on an antibody with variable domains targeted against human insulin receptor (purple), conjugated to imaging agents (stars). (**f**) Boado *et al*. [71] demonstrated Trojan horse-mediated brain delivery of a radiolabeled therapeutic anti-HIR conjugate in nonhuman primates. Autoradiography of postmortem brain sections from a monkey treated with unconjugated agent (left) *vs*. a monkey treated with anti-HIR-conjugated probe (right) illustrate strong brain uptake dependent on the anti-HIR construct. Radiolabel density indicated by yellow-red-back color scale. This technique could be adapted for delivery of MRI contrast agents, although only the most potent agents are likely to be appropriate. Figure adapted from ref. 71.